Photovoltaic Devices

DOI: 10.1002/anie.200902861

Synthesis and Photoelectrochemical Study of Vertically Aligned Silicon Nanowire Arrays**

*Guangbi Yuan, Huaizhou Zhao, Xiaohua Liu, Zainul S. Hasanali, Yan Zou, Andrew Levine, and Dunwei Wang**

Photon absorption, charge separation, and charge collection are key steps involved in photovoltaics.[1] Optimizing and balancing these steps is crucial to maximizing the overall power conversion efficiency, but has been proven to be exceedingly difficult because each step poses unique and conflicting requirements. For example, a thick material is desired for better light absorption, whereas a thin material with short charge-diffusion length is favored for charge collection. Dilemmas like this present great challenges in material synthesis and device fabrication, and keep the cost of efficient devices high. Conversely, devices made with less care fail to offer practical efficiency or durability.[2] To date, energy supplies converted directly from the sunlight remain low despite the obvious advantages, such as renewability, over those from fossil fuels.

From a material and device structure standpoint, high aspect ratio nanowires (NWs) are a promising candidate to convert photons to charges efficiently.[3–5] NWs absorb light in the longitudinal direction ($>1\,\mu m$) and separate and collect charges in the transverse direction (ca. 100 nm), thus easily circumventing the conflicting requirements described above.[4] Moreover, the development of synthetic chemistry has made it possible to produce bulk quantities of NWs inexpensively.[6] For these reasons, immense research efforts have been devoted to realizing efficient power conversion using NWs.[3–5]

The effect of several important parameters of NWs, including length, diameter, and doping level, remain to be experimentally studied for high efficiency solar cells, answers to which are expected to lie in the fundamental photophysical processes.[4] Initial efforts to study these parameters have been exerted primarily on individual NWs.[7] Although highly revealing, the statistical significance of these results when extended to a large number of NWs ($>10^6\,mm^{-2}$) has yet to be evaluated. It is equally important to perform these studies on nanoscale structures. Herein, we report our latest progress toward this goal. We first show that vertical silicon nanowires (SiNWs) can be readily synthesized with excellent alignment under mild conditions. Enabled by this synthetic control, we then systematically varied different parameters of the NWs and studied their influence on the charge behavior in a photoelectrochemical setup. Our results reveal that NWs with diameters close to the width of space charge region perform better than thicker NWs. These results are expected to pave the way for NW-based devices that will harvest solar energy efficiently.

Although they have been extensively studied for electronic applications for nearly a decade,[8] SiNWs have only recently been considered for photovoltaic devices. For photon-to-charge conversion, vertically aligned NW arrays are favored over those in random orientations.[4] In an array of NWs without alignment, the charge transport pathway is inadvertently increased when two NWs are in contact, leading to decreased efficiencies.[9] Existing reactions that produce vertical SiNWs using chemical vapor deposition (CVD) take place either at high temperatures ($>800\,^\circ C$),[10–12] in which both the substrate and the precursor molecules are heated, or at moderate temperatures (400–800 °C) in cold-wall systems, in which only the substrate is heated.[13–15] Little is known about why the same results are rarely obtained in a simple thermal CVD apparatus with SiH_4 as a precursor even though this system has been widely used to produce randomly oriented SiNWs.[8,16] Our first goal was to unravel the causes of the growth difference and thus to develop a synthesis that takes places at mild temperatures without producing hazardous by-products. Achieving this goal serves dual purposes: increasing the understanding of vapor–liquid–solid (VLS) NW growth mechanism, and obtaining products with dimensions and properties desirable for light-to-electricity conversion.

We obtained vertically aligned SiNWs as shown in Figure 1a in a narrow window of growth conditions: $635\,^\circ C < T < 680\,^\circ C$ and $0.5\ Torr < p_{SiH_4} < 1.5\ Torr$; the optimum conditions were $T = 650\,^\circ C$ and $p_{SiH_4} = 1\ Torr$. Conditions outside of this range produced NWs with either random orientations or severe particular depositions or both (see the Supporting Information). Note that crystalline SiNWs, random or aligned, have been produced at a variety of temperatures (290–1200 °C) and pressures (10^{-6}–760 Torr).[12–14,16–18] Nevertheless, the temperature and pressure combination obtained in this study is unique. We understand the difference as follows.

The key to a high degree of vertical alignment is to promote growth of NWs whose axial crystal orientation is

[*] G. Yuan, Dr. H. Zhao, Dr. X. Liu, Z. S. Hasanali, Dr. Y. Zou, A. Levine, Prof. Dr. D. Wang
Department of Chemistry, Boston College
Merkert Chemistry Center
2609 Beacon St., Chestnut Hill, MA, 02467 (USA)
Fax: (+1) 617-552-2705
E-mail: dunwei.wang@bc.edu
Homepage: http://www2.bc.edu/~dwang

[**] This work was supported by Boston College and partially by a DOD subcontract through Agiltron. We thank Dr. D. Z. Wang for his assistance in sample characterizations, and Y. Lin and S. Zhou for helpful discussions.

Supporting information for this article is available on the WWW under http://dx.doi.org/10.1002/anie.200902861.

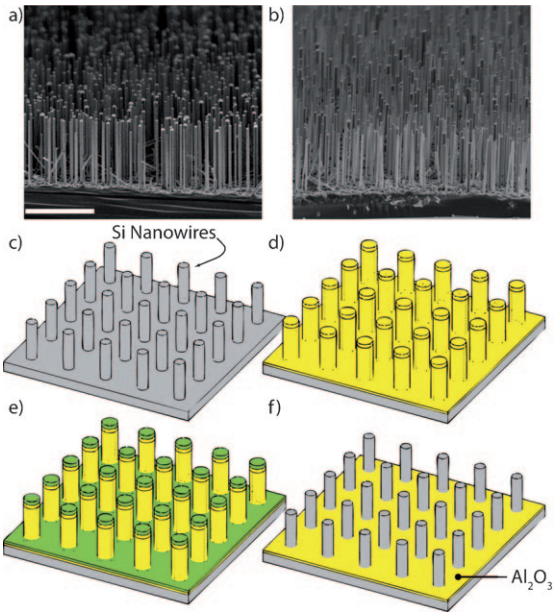

Figure 1. a) SEM pictures of as-synthesized vertical SiNWs; and b) after removal of Au; scale bar: 10 μm. c–f) Fabrication of the photoelectrode. After removal of Au (c), the sample was coated with Al_2O_3 using ALD (d), followed by directional metal coating (e). The fabrication was concluded with Al_2O_3 etching and removal of sacrificial metal (f).

normal to Si substrate surface, and to limit growth of NWs of other axial orientations. For example, to achieve vertical SiNW arrays on a Si(111) substrate, it is necessary to grow them along only one of the four possible ⟨111⟩ directions so that most NWs are normal to the substrate surface.[11,19] In an epitaxial system, the growth of SiNWs normal to the (111) plane is favored over SiNWs along other equivalent ⟨111⟩ directions. The energy difference, however, is subtle. This difference can be utilized to produce SiNWs with uniform axial orientations only when the manner in which Si atoms precipitate out of the liquid alloy seed and are subsequently deposited is carefully controlled. Low reaction rates are generally preferred. Fast Si deposition will otherwise produce NWs with orientations or even crystal structures that are energetically unfavored.[19,20] This understanding is consistent with previous reports, in which vertical SiNWs have been commonly produced using $SiCl_4$[10–12] or using SiH_4 at low pressures.[13,17,19] Under these reported reaction conditions, low Si feeding results in slow growth. Nevertheless, these reactions either take place at high temperatures and produce corrosive by-products (e.g., $SiCl_4$-fed growth) or require costly special equipment (e.g., molecular-beam epitaxy systems). In contrast, a hot-wall CVD system with SiH_4 as precursor is easy to implement and has been widely used to grow randomly oriented SiNWs. Reports on highly aligned SiNW arrays using this system are scarce because reactions in such system are typified by fast growth—too fast to maintain a uniform [111] growth. By growing vertical SiNWs with high degree alignment in a hot-wall CVD system with SiH_4 as feedstock, we show that this challenge can be solved.

Under our growth conditions ($T = 650\,°C$ and $p_{SiH_4} = 1$ Torr), SiH_4 readily decomposes into various silicon hydride species upon entry into the heated zone.[21] The concentration of Si-containing species is the highest in the upstream region, where vertical SiNW growth is unattainable. The concentration decreases downstream, and vertical SiNW growth becomes possible. We obtained vertical SiNWs 17 cm downstream in the heated zone. Consistent with the understanding that low reaction rates favor vertical SiNW growth, this growth is maintained further downstream, albeit at a lower rate (see the Supporting Information). We note that Si atoms are not a direct product of SiH_4 thermal decomposition under our studied conditions. This conclusion is supported by reference [21], as well as by our control experiments (see the Supporting Information). NWs obtained in this study were straight and free of tapering. This fact also supports the hypothesis that no Si atoms are directly produced in the gas phase where vertically aligned SiNWs are grown.

The growth result is significant in two respects. First, it fills in the knowledge gap and explains why vertical SiNWs have rarely been obtained in simple hot-wall CVD systems with SiH_4 as feedstock. Second, it provides us an opportunity to study the photon-to-charge conversion of vertically aligned SiNWs in a photoelectrochemical (PEC) setup.[22] When immersed in a Me_2Fc^+/Me_2Fc (1:400) solution in methanol (Me_2Fc = dimethylferrocene), the SiNW Fermi level equilibrates with the electrochemical potential of the redox pair, leading to band bending (Figure 2). The gradient represents

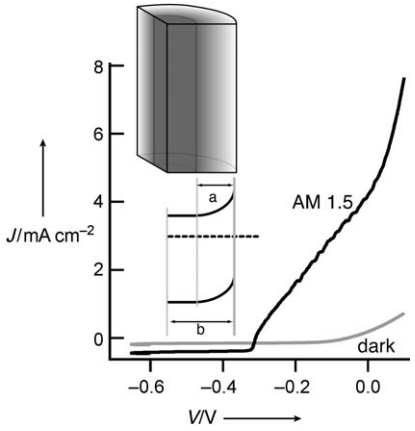

Figure 2. Current vs. voltage plot for SiNW photoelectrodes measured in a Me_2Fc^+/Me_2Fc electrolyte in the dark and under simulated sunlight (air mass (AM) 1.5). The corresponding energy diagram of an n-type NW is shown in the inset; *a* denotes the width of the space charge region and *b* is the radius of the NW.

electron density in different regions of a NW, the highest in the center and the lowest at the surface. The region with band bending is also known as the space charge region where photogenerated electrons and holes are separated. Electrons are concentrated into the center to be transported, and holes are transferred to the solution to oxidize Me_2Fc. This setup is simple to construct and powerful in characterizing the intrinsic electronic properties of semiconductors.[23]

Electrons are the majority charge carrier in n-type Si. Their transferring to the solution for Me_2Fc^+ reduction is prohibited by the existence of the barrier as a result of band bending (Figure 2, inset). In contrast, although holes can be readily transferred to the solution to oxidize Me_2Fc, their density is low in n-type Si. As a result, this transfer mechanism contributes little to the overall current flow in the absence of light. Indeed, only limited current was observed when the cell was measured in dark (Figure 2). The hole density increases dramatically when Si is exposed to simulated sunlight as a result of charge excitation. Photogenerated holes are subsequently collected and concentrated in the space charge region and then transferred to the electrolyte. A current was measured with no or low negative applied bias (Figure 2). A more negative bias shifts the Si electronic potential upward, reducing the width of the space charge region and eventually stopping the current flow. In analogy to a solid-state p/n junction, the potential at $I=0$ is denoted as V_{oc}, representing the open-circuit voltage, and the current at $V=0$ is denoted as I_{sc}, representing the short-circuit current. We note that in practice the Si/Me_2Fc junction is an intricate system. I_{sc} and V_{oc}, however, are fundamentally important parameters that provide quantitatively significant comparisons of the NW electrode performance in harvesting solar energy.[1,24] Choosing them as a benchmarking basis suffices our purposes for the systematical comparison of various SiNWs as photoelectrodes.

The values of I_{sc} and V_{oc} for the Si/Me_2Fc junction are sensitive to a number of factors, including light intensity, doping level (hence the physical dimension of the space charge region), and charge traps. Because we grew SiNWs on crystalline Si substrates, it was necessary to eliminate any potential contribution from the supporting substrate. For this purpose, we used Al_2O_3 to cover the support substrate (Figure 1 c–f). In the resulting electrode, only vertical SiNWs are exposed to the electrolyte. A platform to systematically study SiNWs as photoelectrodes is thereby obtained.

Our next study focused on varying the NW doping level, length, and diameter and observing how the changes effect the photon-to-charge conversion. The experimental design was guided by the following principles. First, longer NWs are able to absorb more photons and thus generate more charges. This advantage competes with the drawbacks that more charge traps and scatter centers are also present in longer NWs. Thus, one expects to observe an optimum length for maximum photocurrents (I_{sc}).[25] Second, the NWs should not be significantly wider than the space charge region (10^1–10^2 nm for moderately doped Si), in which charge collection efficiency is near unity. Although minority charge carriers can diffuse for up to several micrometers in moderately doped Si, charge separation and collection only occur in the space charge region. Maximum charge collection efficiency is therefore expected for NWs with diameters in the nanoscale region. Competing with the tendency to keep NWs small is the consideration of surface state density. Surface states, more concentrated in smaller NWs, reduce photocurrents through recombination and scattering. Therefore, an optimum diameter is expected. Third, a more heavily doped NW transports majority charge carriers better, but negates minority carrier diffusion. Ideally, the doping level should yield a nearly depleted NW for efficient charge collection with the core region spared for effective majority charge transporting (Figure 2 inset). Taken as a whole, maximum photocurrent is expected for samples consisting of moderately doped NWs that are 10–30 μm long and 200–300 nm in diameter. We now discuss the influence of these parameters on the photon-to-charge conversion.

Figure 3 shows the photocurrents obtained for SiNWs with different lengths. The photocurrent density was calculated on the basis of the overall projected area. Note that only

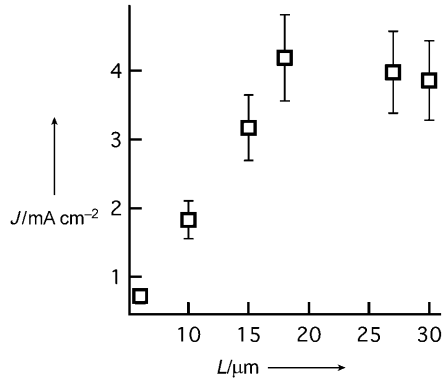

Figure 3. Photocurrent dependence on NW lengths.

around 7% of the substrate was covered by SiNWs. If no contribution from the void region (covered by Al_2O_3) is taken into account, the photocurrent density could be increased by greater than 10-fold. As shown in Figure 3, higher I_{sc} values were observed for photoelectrodes consisting of longer NWs because they absorb more light. A maximum value for I_{sc} was measured for samples consisting of NWs around 18 μm long. Further increases in NW length led to a decrease in the I_{sc} value as a result of increased charge scattering and recombination. A consistent trend was also observed for the V_{oc} value. Similar to I_{sc}, V_{oc} is sensitive to absorbed photon influx as well as surface states. Within the measurement accuracy, the V_{oc} values were relatively stable and exhibited a trend to decrease when NWs became longer. The decrease is caused by the increase of surface states per unit illumination area (Table 1).

Table 1: Dependence of V_{oc} on NW length.

L [μm]	6	10	15	18	27	30
V_{oc} [mV]	313 ± 45	344 ± 51	322 ± 48	310 ± 45	301 ± 45	267 ± 40

It is noteworthy that the I_{sc} values obtained in this study are higher than for microscale Si wires,[3] but lower than for bulk Si crystals (see the Supporting Information). We suggest that future research be directed toward increasing NW coverage and reducing surface states to improve NW-based photon-to-charge conversion.

The I_{sc} and V_{oc} values measured for SiNWs with different doping levels are given in Table 2. The doping level was varied by changing the SiH_4/PH_3 ratio during the synthesis. Micro-

Table 2: Influence of doping level on values of V_{oc} and I_{sc}.

Doping level [cm^{-3}]	10^{10}	10^{14}	10^{16}	10^{18}
I_{sc} [$mA\,cm^{-2}$]	0.44 ± 0.10	1.2 ± 0.20	2.37 ± 0.35	4.19 ± 0.60
V_{oc} [mV]	56 ± 10	308 ± 45	337 ± 50	310 ± 45

electrodes were fabricated in a four-probe fashion to contact individual NWs to measure the electrical resistance, which was then used to calculate the doping level. The measured I_{sc} values increase monotonically with the increase in the NW doping level. The highest I_{sc} value was obtained for SiNWs with a doping level of $10^{18}\,cm^{-3}$. For all data shown in Table 2, the NW dimensions (200 nm wide and 18 μm long) and surface coverage (7% coverage of the illuminated area) were identical. Thus, the density of photogenerated charges is comparable. SiNWs with lower doping level generated lower I_{sc} values as a result of poorer electrical conductivity. Further increase of dopant densities, however, is expected to reduce the space charge region and the diffusion distance of minority carrier, consequently leading to lower I_{sc} values.[4] As we were limited by growth constraints, we were unable to produce SiNWs with dopant densities greater than $10^{18}\,cm^{-3}$ to verify this hypothesis experimentally.

The last studied parameter was NW diameter (Table 3). SiNWs of the same length (18 μm) and the same surface coverage (ca. 7%) were used for these measurements. Within

Table 3: Influence of NW diameter on values of V_{oc} and I_{sc}.

NW diameter [nm]	200	150	80
I_{sc} [$mA\,cm^{-2}$]	4.19 ± 0.60	4.85 ± 0.72	1.84 ± 0.28
V_{oc} [mV]	310 ± 45	324 ± 50	328 ± 50

the measurement accuracy, comparable I_{sc} and V_{oc} values were obtained on SiNWs with $d\approx200$ and 150 nm. The space charge region is approximately 30 nm for Si with a doping level of $10^{18}\,cm^{-3}$ and a surface potential of approximately 300 mV (caused by Me_2Fc/Me_2Fc^+ electrolyte). A core of around 140 nm for a 200 nm wide NW (ca. 90 nm for a 150 nm wide NW) is unaffected by the surface potential. The unaffected core is only about 20 nm wide for an 80 nm wide NW, which is too thin to transport charges efficiently. As a result, a much smaller I_{sc} value was measured for 80 nm wide NWs than for 150 or 200 nm wide ones (Table 3). Note that the current reduction may also be attributed to other factors, such as a smaller total projected area for smaller NWs or a higher density of surface states. These factors were determined to be insignificant, as the V_{oc} values were relatively stable (Table 3).

Finally, we emphasize that the measurements were highly sensitive to sample quality, mainly how well SiNWs were aligned. Significantly lower I_{sc} and V_{oc} values than those reported herein were obtained when the alignment was inferior to that shown in Figure 1a. In addition to increased charge transport pathway, the imperfection in alignment also led to device fabrication defects. Once good alignment was achieved, the results were highly reproducible. The reported data were reproduced in more than 50 batches of samples. Caution was taken to evaluate the alignment using SEM prior to electrode fabrication and characterization.

In summary, we developed a synthesis to fabricate vertically aligned SiNW arrays using simple thermal CVD systems and SiH_4 as a precursor. The key to our success was to maintain a low Si feeding rate to achieve a slow growth. The growth control enabled us to study systematically the prospect of using SiNWs for photovoltaic devices. Our results showed that efficient energy conversion was achieved for SiNWs with high degree of alignment, doped at around $10^{18}\,cm^{-3}$, and around 20 μm long and 200 nm wide. The results agree well with previous theoretical studies, thus experimentally validating SiNWs as a promising candidate for efficient solar-energy harnessing.

Experimental Section

SiNW synthesis: An n-type Si (111) substrate (10–40 Ω cm, Wafternet) was cleaned sequentially in acetone, methanol, and isopropanol and then etched in buffered oxide etchant (BOE, 7:1, J.T. Baker) for 2 min. Gold (6 nm thick) was then evaporated to serve as growth seeds. The growth was carried out in a home-built CVD apparatus with automatic flow and pressure controls. In a typical growth procedure, the substrate was placed 1–2 cm downstream from the furnace center (ca. 17 cm from where the heating started) in a quartz tube. It was first annealed at 900 °C for 10 min with 60 sccm (standard cubic centimeter per minute) H_2 flow at $p_{total}=500$ mTorr. The temperature was then decreased to 650 °C, and the gas flow was changed to 120 sccm PH_3 (150 ppm in H_2) and 60 sccm SiH_4 (10% in He) at $p_{total}=20$ Torr. The length of the NWs was controlled by adjusting the reaction duration and it was found to follow a linear dependence of approximately 9 $\mu m\,h^{-1}$.

Photoelectrode fabrication: The substrate covered by SiNW arrays was etched in 2% HF for 1 min and then immersed in thin film etchant type A (Transene) for 25 min to remove Au. The effectiveness of this process was confirmed by using a scanning electron microscope (JSM-6340F) equipped with elemental analysis capabilities. The sample was then annealed in a rapid thermal processing (RTP) system in forming gas at 900 °C for 30 s to fix surfaces damaged during previous wet etching steps. The RTP annealing was found to be crucial. Afterwards, a 100 nm Al_2O_3 film was deposited in a Cambridge nanotech atomic layer deposition (ALD, Savannah 100) system. An Au film (90 nm) was evaporated along the NW standing direction so that it only covered the NW tips and the regions without NWs. Finally, TRANSETCH-N (Transene) was used to remove Al_2O_3 on the side wall and tip of the NWs (180 °C, 9 min). The fabrication was concluded by the removal of the Au protection layer with etchant. The resulting photoelectrode had only vertical SiNWs exposed, and the rest were covered in Al_2O_3.

PEC measurements: PEC measurements were conducted using a CHI 600C potentiostat/galvanostat in a three-electrode configuration. The electrolyte solution contained 200 mM dimethylferrocene (Me_2Fc) (97%, Alfa Aesar), 0.5 mM Me_2FcBF_4, and 1M $LiClO_4$ (>99%, Fisher) in methanol (99.9%, Fisher). All reagents were used as received without further purification except for $Me_2Fc^+BF_4^-$, which was synthesized by a published method.[26] Stoichiometric amounts of solid $AgBF_4$ and Me_2Fc were added to anhydrous acetone (10 mL). Ag, in the form of dark gray precipitate, was removed by filtration, and $Me_2Fc^+BF_4^-$ was collected by solvent evaporation and dried under vacuum. For all data reported herein, simulated sunlight ($100\,mW\,cm^{-2}$, AM 1.5, Oriel 96000) was used as the light source. All

data were recorded at a scan rate of 100 $mV s^{-1}$. Voltage corrections were performed to eliminate the influence of series resistance.[27]

Received: May 28, 2009
Revised: September 25, 2009
Published online: November 13, 2009

Keywords: chemical vapor deposition · energy conversion · nanostructures · solar cells

[1] J. Nelson, *The Physics of Solar Cells*, Imperial College Press, Longdon, **2003**.
[2] N. S. Lewis, *Science* **2007**, *315*, 798.
[3] J. R. Maiolo, B. M. Kayes, M. A. Filler, M. C. Putnam, M. D. Kelzenberg, H. A. Atwater, N. S. Lewis, *J. Am. Chem. Soc.* **2007**, *129*, 12346.
[4] B. M. Kayes, H. A. Atwater, N. S. Lewis, *J. Appl. Phys.* **2005**, *97*, 114302.
[5] A. P. Goodey, S. M. Eichfeld, K. K. Lew, J. M. Redwing, T. E. Mallouk, *J. Am. Chem. Soc.* **2007**, *129*, 12344; B. Tian, X. Zheng, T. J. Kempa, Y. Fang, N. Yu, G. Yu, J. Huang, C. M. Lieber, *Nature* **2007**, *449*, 885; E. C. Garnett, P. Yang, *J. Am. Chem. Soc.* **2008**, *130*, 9224.
[6] D. W. Wang, Y. L. Chang, Z. Liu, H. J. Dai, *J. Am. Chem. Soc.* **2005**, *127*, 11871; M. Law, J. Goldberger, P. D. Yang, *Annu. Rev. Mater. Res.* **2004**, *34*, 83.
[7] B. Tian, T. J. Kempa, C. M. Lieber, *Chem. Soc. Rev.* **2009**, *38*, 16; T. J. Kempa, B. Z. Tian, D. R. Kim, J. S. Hu, X. L. Zheng, C. M. Lieber, *Nano Lett.* **2008**, *8*, 3456; M. D. Kelzenberg, D. B. Turner-Evans, B. M. Kayes, M. A. Filler, M. C. Putnam, N. S. Lewis, H. A. Atwater, *Nano Lett.* **2008**, *8*, 710.
[8] C. M. Lieber, *Mater. Res. Bull.* **2003**, *28*, 486.
[9] K. Zhu, T. B. Vinzant, N. R. Neale, A. J. Frank, *Nano Lett.* **2007**, *7*, 3739.
[10] R. S. Wagner, W. C. Ellis, *Appl. Phys. Lett.* **1964**, *4*, 89.
[11] S. P. Ge, K. L. Jiang, X. X. Lu, Y. F. Chen, R. M. Wang, S. S. Fan, *Adv. Mater.* **2005**, *17*, 56.
[12] A. I. Hochbaum, R. Fan, R. R. He, P. D. Yang, *Nano Lett.* **2005**, *5*, 457.
[13] J. Westwater, D. P. Gosain, S. Tomiya, S. Usui, H. Ruda, *J. Vac. Sci. Technol. B* **1997**, *15*, 554.
[14] Y. W. Wang, V. Schmidt, S. Senz, U. Gosele, *Nat. Nanotechnol.* **2006**, *1*, 186.
[15] J. B. Hannon, S. Kodambaka, F. M. Ross, R. M. Tromp, *Nature* **2006**, *440*, 69.
[16] K. K. Lew, J. M. Redwing, *J. Cryst. Growth* **2003**, *254*, 14; H. Z. Zhao, S. Zhou, Z. Hasanali, D. W. Wang, *J. Phys. Chem. C* **2008**, *112*, 5695.
[17] J. B. Hannon, S. Kodambaka, F. M. Ross, R. M. Tromp, *Nature* **2006**, *440*, 69.
[18] J. Y. Yu, S. W. Chung, J. R. Heath, *J. Phys. Chem. B* **2000**, *104*, 11864; Y. Cui, L. J. Lauhon, M. S. Gudiksen, J. F. Wang, C. M. Lieber, *Appl. Phys. Lett.* **2001**, *78*, 2214; P. Qi, W. S. Wong, H. Zhao, D. Wang, *Appl. Phys. Lett.* **2008**, *93*, 163101.
[19] A. Lugstein, M. Steinmair, Y. J. Hyun, G. Hauer, P. Pongratz, E. Bertagnolli, *Nano Lett.* **2008**, *8*, 2310.
[20] A. F. I. Morral, J. Arbiol, J. D. Prades, A. Cirera, J. R. Morante, *Adv. Mater.* **2007**, *19*, 1347; X. H. Liu, D. W. Wang, *Nano Res.* **2009**, *2*, 575; G. Yuan, X. Liu, W. He, D. Wang, *Appl. Phys. A* **2009**, *96*, 399; S. N. Mohammad, *Nano Lett.* **2008**, *8*, 1532.
[21] A. A. Onischuk, V. P. Strunin, M. A. Ushakova, V. N. Panfilov, *Int. J. Chem. Kinet.* **1998**, *30*, 99.
[22] M. X. Tan, P. E. Laibinis, S. T. Nguyen, J. M. Kesselman, C. E. Stanton, N. S. Lewis, *Prog. Inorg. Chem.* **1994**, *41*, 21.
[23] C. M. Gronet, N. S. Lewis, G. Cogan, J. Gibbons, *Proc. Natl. Acad. Sci. USA* **1983**, *80*, 1152.
[24] S. K. Haram, *Semiconductor Electrodes*, Elsevier, New York, **2007**; Y. V. Pleskov, *Solar Energy Conversion: A Photoelectrochemical Approach*, Springer, New York, **1990**.
[25] H. Fang, X. D. Li, S. Song, Y. Xu, J. Zhu, *Nanotechnology* **2008**, *19*, 255703.
[26] G. Tabbi, C. Cassino, G. Cavigiolio, D. Colangelo, A. Ghiglia, I. Viano, D. Osella, *J. Med. Chem.* **2002**, *45*, 5786.
[27] J. R. Maiolo, H. A. Atwater, N. S. Lewis, *J. Phys. Chem. C* **2008**, *112*, 6194.

